PAPER

Check for updates

Self-induced transformation of raw cotton to a nanostructured primary cell wall for a renewable antimicrobial surface

Sunghyun Nam, [ID] * Matthew B. Hillyer, [ID] Zhongqi He, [ID] SeChin Chang [ID] and J. Vincent Edwards

Herein, raw cotton is shown to undergo self-induced transformation into a nanostructured primary cell wall. This process generates a metal nanoparticle-mediated antimicrobial surface that is regenerable through multiple washings. Raw cotton, without being scoured and bleached, contains noncellulosic constituents including pectin, sugars, and hemicellulose in its primary cell wall. These noncellulosic components provide definitive active binding sites for the *in situ* synthesis of silver nanoparticles (Ag NPs). Facile heating in an aqueous solution of $AgNO_3$ activated raw cotton to produce Ag NPs (*ca.* 28 nm in diameter and 2261 mg kg^{-1} in concentration). Compared with scoured and bleached cotton, raw cotton requires lower concentrations of $AgNO_3$—ten times lower for *Klebsiella pneumonia* and two times lower for *Staphylococcus aureus*—to achieve 99.9% reductions of both Gram-positive and Gram-negative bacteria. The Ag NPs embedded in the primary cell wall, which was confirmed *via* transmission electron microscopy images of the fiber cross-sections, are immobilized, exhibiting resistance to leaching as judged by continuous laundering. A remarkable percentage (74%) of the total Ag NPs remained in the raw cotton after 50 laundering cycles.

Introduction

Nanotechnology has the potential to improve processes, materials, and applications.[1–3] The textile industry is no exception to this. Various functional nanoparticles have been applied to textiles to develop products that exhibit advantageous antibacterial activity, stain repellence, and static elimination.[4,5] However, the complete realization of nanotechnology in the textile industry has been hampered by the high cost and complexity of nanoparticle synthesis. Methods for synthesizing nanoparticles require the use of several chemical agents, including reducing agents to convert the precursor metal ions into metal atoms and stabilizing agents to prevent particle agglomeration. In some cases, solvents, *e.g.*, ethylene glycol are required.[6,7] Commonly used reducing agents, such as hydrazine, sodium borohydride, and *N,N*-dimethylformamide, are associated with environmental and biological hazards.[8,9] Moreover, determination of the optimal ratios between agents and precursors, which is critical to controlling particle growth at the nanoscale, is a complex process.[10,11]

Fixating individual nanoparticles onto textiles is a challenge for producing reliable nano-enhanced textile products. Current fixation practices include applying nanoparticles to textiles using chemical binders and introducing chemical bonds between the nanoparticles and surface of textiles.[12,13] During the application, numerous nanoparticles aggregate into large particles. Studies have shown that the particles observed on the textile surfaces were up to two orders of magnitude larger than the original particles in the colloidal solution before the application.[14–16] The aggregated particles would lose any benefits associated with their nanosized counterparts. Additional fixation processes, involving multiple chemical reactions, can alter the intrinsic feel of the textile materials.

Another challenge is that textile products, unlike other consumer products, undergo routine washing. As machine washing imposes remarkable mechanical and chemical impacts on the textiles, most nanoparticles applied to the textiles are washed away. For example, the silver nanoparticle (Ag NP)-induced odor-inhibiting or anti-infective textile products on the market are not durable. Socks emit up to 25% of the total Ag into the detergent solution during a single machine wash[17,18] and almost 100% into distilled water during four sequential 24 h gentle agitations.[19] Shirts and trousers lose 18% of the total Ag after a single machine washing cycle in a detergent solution[17] and 2% after a 1 h agitation in tap water.[20] Medical textiles such as masks and clothes lose 23–27% after a 1 h agitation in tap water.[20]

Herein, an ecofriendly, economical, and reliable approach to the Ag NP functionalization of textiles was proposed. Because textile finishing is partially responsible for global

U.S. Department of Agriculture, Agricultural Research Service, Southern Regional Research Center, New Orleans, LA 70124, USA. E-mail: sunghyun.nam@usda.gov; Fax: +1 504 286 4390; Tel: +1 504 286 4229

environmental pollution, there have been several efforts to develop "green" finishing techniques.[21–25] These approaches include fabricating multifunctional textile coatings that impart several properties, such as flame retardancy, hydrophobicity, and antimicrobial properties to textiles using biopolymers based on rice husk,[22] rennet casein,[24] and molokhia.[25] Here, the proposed approach is based on the ability of raw cotton to produce Ag NPs by itself. The primary cell wall of cotton fiber, which contains noncellulosic constituents such as pectin, sugars, fatty alcohols, and hemicellulose, serves as a nanoreactor. Almost all cotton fibers in the textile industry are scoured and bleached (SB); however, these processes have negative impacts on the environment. They consume large amounts of water, energy, and chemicals, and they cause high chemical oxygen demand and high biological oxygen demand in textile effluents.[26] In the case of hydrogen peroxide bleaching, chemical, energy, and water consumptions are estimated to be 0.118 kg kg^{-1} textiles, 8.34 MJ kg^{-1} textiles, and 50 L kg^{-1} textiles, respectively.[27] Therefore, using raw cotton as a tool to produce Ag NPs increases the economical and ecofriendly advantages of the proposed approach.

Another beneficial aspect of this approach is that it does not require reducing or stabilizing agents. Raw cotton fiber can self-form a nanostructured internal layer without the need for external agents or chemical modifications to the cotton fiber. To demonstrate this unique capability of raw cotton, it was compared with SB cotton fiber by measuring the optical properties of the cotton fiber using transmission electron microscopy (TEM) images of the cross-section of the fiber, monitoring the development of the surface plasmon resonance (SPR) of Ag NPs over the reaction time, and assessing the antimicrobial properties of the fibers. Finally, the durability of Ag NPs embedded in the primary cell wall was examined by performing multiple launderings.

Experimental section

Materials

The commercially available mechanically pre-cleaned raw white cotton fiber was obtained from T. J. Beall (Greenwood, MS, USA). Commercially available scoured and bleached (SB) white cotton fiber was obtained from Barnhardt Manufacturing Co. (Charlotte, NC, USA). Scoured, bleached, and desized white cotton print cloth (98 g m^{-2}) and raw white cotton print cloth (122 g m^{-2}) were purchased from Testfabrics, Inc. (West Pittston, PA, USA). The raw cotton print cloth was desized before treatment. Silver nitrate (AgNO$_3$, 99.9%) was purchased from J. T. Baker (Radnor, PA, USA). Triton X-100, polysorbate 80, methyl methacrylate, butyl methacrylate, and methyl ethyl ketone were purchased from Sigma-Aldrich (St. Louis, MO, USA). All chemicals were used as received without further purification. Deionized (DI) water was used as a solvent.

Ag NP synthesis by cotton

A 150 mL aqueous solution containing AgNO$_3$ (5 mM) and Triton X-100 (0.05 wt%) was prepared in a 500 mL three-neck round bottom flask. About 1 g of cotton fiber or cotton fabric was immersed in the solution. To monitor the production of Ag NPs in the reaction solution, the flask was equipped with a condenser and sealed with rubber septa. The sample in the solution was heated at 100 °C for 0.25–2 h. Over the course of the reaction, a 2.5 mL reaction solution was collected every 5 min using a syringe needle for the UV/vis analysis. At reaction times selected for this study, the cotton sample was removed from the solution, washed in DI water multiple times, and air-dried.

Characterization

Photographs of samples were taken using a digital camera (RX100, Sony). The optical microscopic images of fibers in the longitudinal view were collected using a digital microscope (KH-8700, Hirox).

The cross-section of cotton fiber was observed by transmission electron microscopy (TEM, JEM-2010, Jeol) operating at 200 kV. For the preparation of cross-sectioned fibers, a bundle of fibers randomly collected was combed and embedded in a mixture of methyl methacrylate and butyl methacrylate, which was polymerized using a UV cross-linker (UVP, CL-1000) for 30 min following the published techniques.[28,29] A block of the fiber bundle was cut into approximately 100 nm-thick slices using a PowerTome Ultramicrotome (Boeckeler Instruments, Inc.), which were placed on a carbon-film-coated copper grid. The embedding medium was removed using methyl ethyl ketone. The size of Ag NPs was determined by the analysis of multiple micrographs using Image J software.[30]

X-ray diffractograms (XRD) were recorded using a diffractometer (XDS 2000, Scintag Inc.) with Cu Kα radiation (0.15406 nm) and the generator working at 43 kV and 38 mA. Angular scanning was conducted from $5°$ to $80°$ at $0.6°$ min^{-1}. The size of crystals was calculated by the Scherrer equation.[31,32]

$$\tau = \frac{K\lambda}{\beta \cos\theta} \tag{1}$$

where K is the correction factor (0.9 for cellulose and 0.94 for Ag NP), λ is the wavelength of the X-ray radiation (1.54056 Å), β is the FWHM of the diffraction peak in radians, and θ is the diffraction angle of the peak.

Ultraviolet/visible (UV/vis) spectra were collected using a UV/vis spectrometer (ISR-2600, Shimadzu) equipped with an integrating sphere unit. Absorbance spectra were collected in a wavelength range of 220–1200 nm. Diffuse reflectance spectra were also recorded in a wavelength range of 380–780 nm to obtain the CIELAB color coordinates—L^*, a^*, and b^*—using UV-2401PC Color Analysis software. L^* represents the lightness of the color ($L^* = 0$ indicates black and $L^* = 100$ indicates white), a^* represents the relative position between red and green (a negative value indicates green while a positive value indicates red), and b^* represents the relative position between yellow and blue (a negative value indicates blue and a positive value indicates yellow). The color difference (ΔE^*) from the reference sample (control cotton) was calculated using the following equation:

$$\Delta E^* = \sqrt{\left(L^* - L_r^*\right)^2 + \left(a^* - a_r^*\right)^2 + \left(b^* - b_r^*\right)^2} \qquad (2)$$

where L^*, a^*, and b^* are the color coordinates for the tested sample, and L_r^*, a_r^*, and b_r^* are the coordinates for the reference sample. The average value of five measurements was presented.

The concentration of Ag was determined using an inductively coupled plasma mass spectrometer (ICP-MS) in the ICP-MS Metals Laboratory at the University of Utah. Approximately 0.05 g of the sample was treated with 2 mL of 16 M nitric acid (trace metal grade) and digested in a Milestone Ethos microwave system. The digest was diluted by weight 1:10, and 10 ppb of indium as an internal standard was added. The digested solution was analyzed with an external calibration curve obtained using a silver single element standard (Inorganic Ventures).

Washing test

Washing in the laboratory machine, Launder-Ometer (M228-AA, SDL Atlas LLC), was conducted following the AATCC Test Method 61-2007: colorfastness to laundering: accelerated. A stainless-steel canister containing 200 mL of detergent solution (0.37 wt% in DI water) and ten stainless steel balls (6.35 mm in diameter), which simulate friction during laundering, was preheated to 45 ± 1 °C in the washing machine. A rectangular fabric specimen (50 mm × 100 mm) was added into the pre-heated canister and rotated at the constant temperature of 40 ± 1 °C with a constant rate of 40 ± 2 rpm for 45 min. This accelerated washing procedure is equivalent to five home or commercial laundering cycles. After washing, the specimen was rinsed in DI water at room temperature for 5 min and air-dried.

Antibacterial properties

Antibacterial properties against Gram-negative *Klebsiella pneumonia* (*K. pneumonia*) and Gram-positive *Staphylococcus aureus* (*S. aureus*) were tested following the AATCC test method 100-2004: "Antibacterial Finishes on Textile Materials: Assessment of" with modification. A concentrated bacterium inoculum was prepared using a spectrophotometer and diluted with sterile water containing a wetting agent (polysorbate 80, 3 wt%). The resulting viable counts for *K. pneumonia* and *S. aureus* were 1.25×10^5 CFU mL^{-1} and 2.31×10^5 CFU mL^{-1}, respectively. The amount of cotton fiber tested was 0.15 g, which absorbed 1 mL of inoculum and left no free liquid. The sample with the inoculum was incubated for 30 min (contact time) at 37 ± 2 °C. Then 100 mL sterile water was added to the sample, which was shaken for 1 min. Serial dilutions of 10^0, 10^1, and 10^2 were made with sterile water, and a 50 mL aliquot was plated on nutrient agar. All plates were incubated for 18 hours at 37 ± 2 °C, and bacterial colonies were counted. Three duplications of each test were conducted. The percent reduction in bacteria was obtained using the following equation:

$$\text{Percent reduction } (\%) = \left(\frac{B - A}{B}\right) \times 100 \qquad (3)$$

where A is the number of viable test bacteria on the test sample after the contact time, and B is the number of viable test bacteria on the control sample immediately after inoculation.

Results and discussion

Raw cotton fibers are slightly yellow because they contain a trace amount of natural pigment (Fig. 1a). This pigment is generally removed by bleaching using hydrogen peroxide. Raw cotton fibers also contain other noncellulosic constituents such as wax, pectin, sugars, proteins, and inorganic salts (metals), which represent approximately 5% of the total weight (dry weight) of typical cotton fibers. The noncellulosic materials can be removed to trace levels by a scouring process using an alkaline sodium hydroxide solution. After the removal of the naturally occurring noncellulosic materials, the cellulose content of the fiber reaches >99%. The SB cotton is white (Fig. 1b) and is used
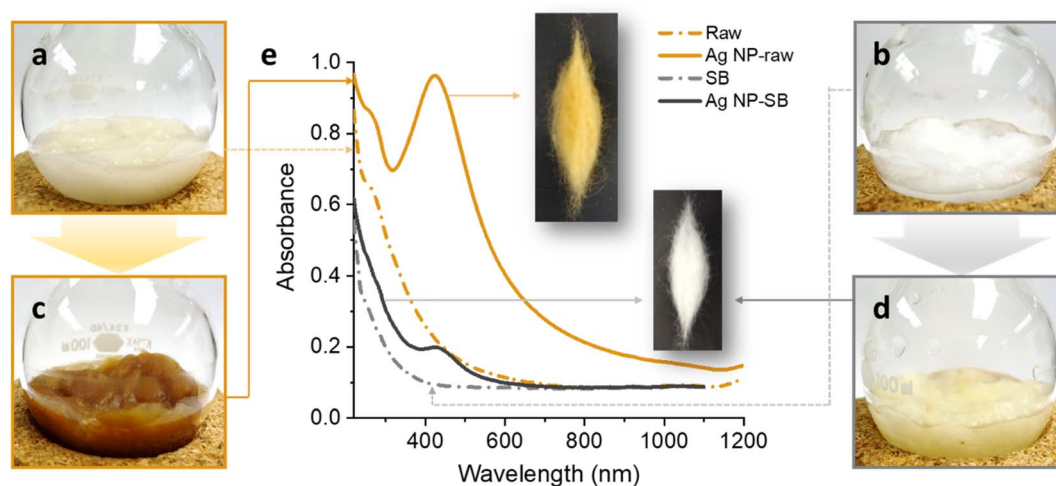

Fig. 1 Photographs of (a) raw and (b) SB cotton fibers before the heat treatment. Photographs of (c) raw and (d) SB cotton fibers after the heat treatment at 100 °C for 2 h. (e) Corresponding UV/vis spectra of the raw and SB cotton fibers. The insets show photographs of the treated raw and SB cotton fiber bundles after washing and air-drying.

in the fabrication of most textile products. Due to the negative impacts of scouring and bleaching processes on the environment, using non-scoured, non-bleached raw cotton fiber is receiving growing attention.[33] Raw cotton fiber can be purified by reginning and lint cleaning without using water or chemicals.[34] This mechanical cleaning reduces the total aerobic yeast and mold count by 99%.[35]

A simple one-step process generated Ag NPs from raw cotton without using any agents. When the raw cotton fiber was heated in an aqueous solution of $AgNO_3$ at 100 °C, the color of the fiber changed to brown within approximately 5 min. Fig. 1c shows a photograph of the raw cotton fiber heated for 2 h. Under the same heat treatment, the color change in the SB cotton fiber was less noticeable (Fig. 1d). Fig. 1e shows the UV/vis spectra of raw and SB cotton fibers before and after heat treatment at 100 °C for 2 h. The insets show the corresponding treated fibers after

washing and drying. After the heat treatment, raw cotton exhibited a strong and distinctive UV/vis peak at approximately 420 nm, which is assigned to the surface plasmon resonance (SPR) of Ag NPs. The SPR of Ag NPs is induced by the interaction of the conduction electrons with the incoming electromagnetic light wave. The SPR peak of the SB fiber was detectable but very weak.

This remarkable change in color and the development of intense SPR indicate that raw cotton fiber can produce Ag NPs. No external agents, *i.e.*, reducing and stabilizing agents were used in this *in situ* synthesis. The comparison results of the SB fiber suggest that the constituents that do not exist in the SB cotton fiber, *i.e.*, noncellulosic constituents contribute to the production of Ag NPs. Some noncellulosic constituents, such as pectin, fatty alcohols, and sugars, can act as a reducing agent, converting Ag cations into Ag atoms. Fig. 2 shows the schematic
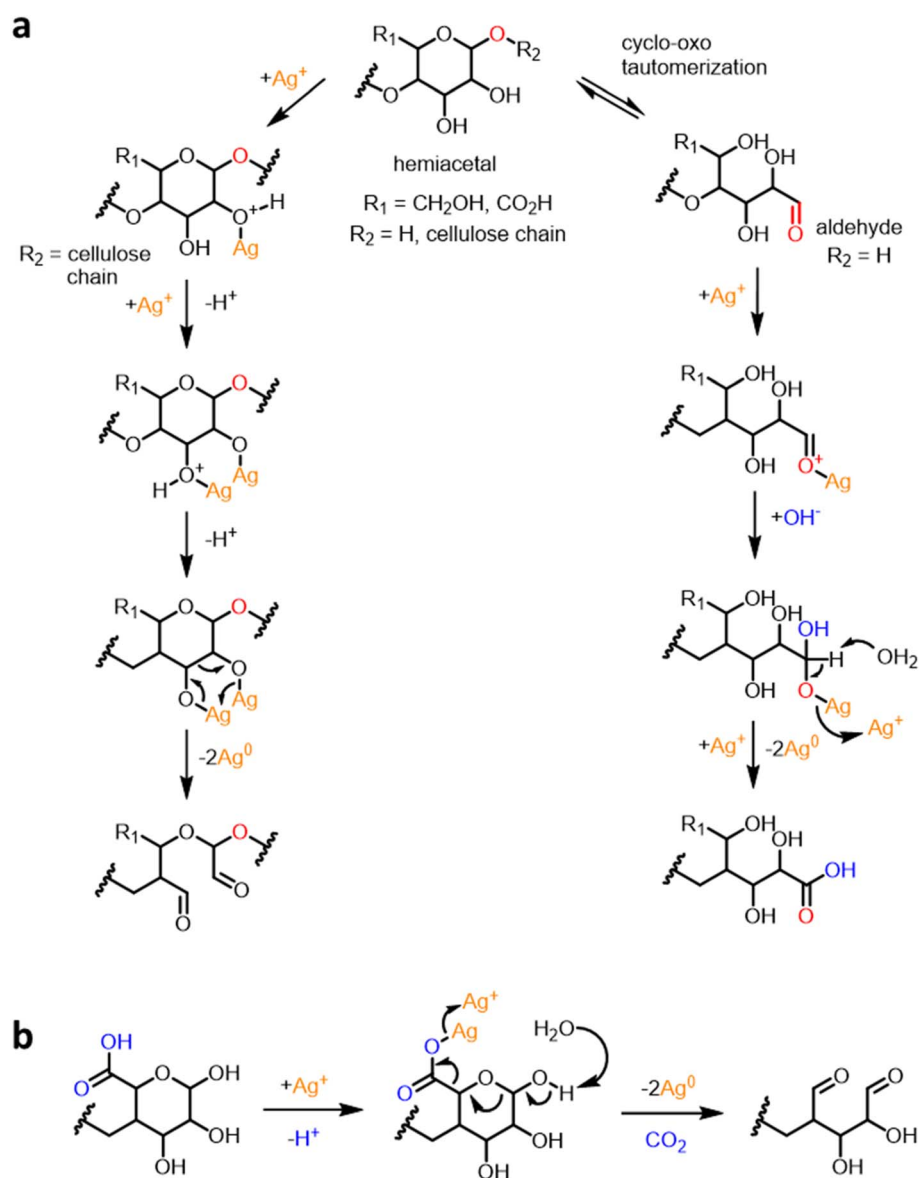

Fig. 2 Schematic diagrams of the reduction reactions of Ag ions by (a) cotton cellulose and pectin and (b) pectin.
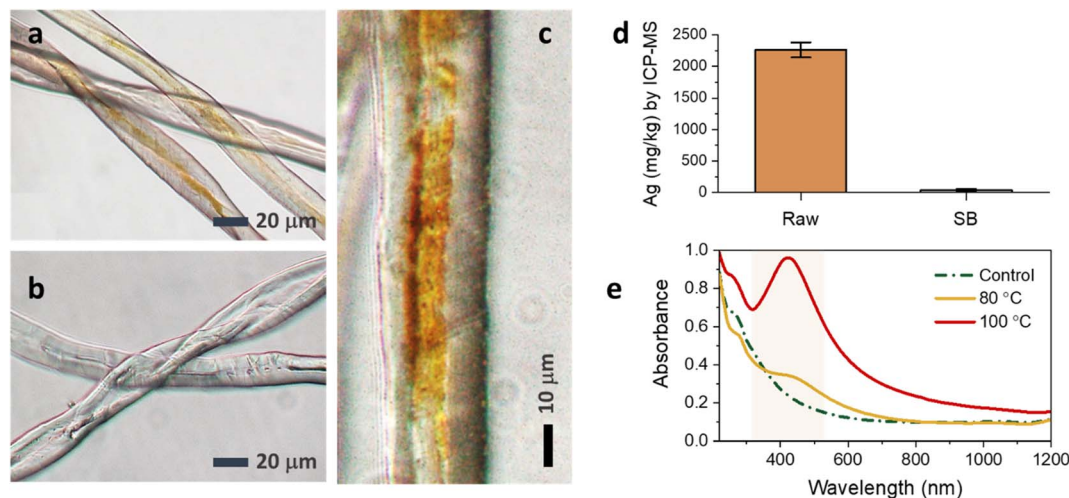
Fig. 3 Optical microscopic images of the longitudinal views of (a) raw and (b) SB cotton fibers obtained after the heat treatment at 100 °C for 2 h. (c) High-magnification optical image of a single Ag NP-raw cotton fiber. (d) Concentrations of Ag based on the dry weights of raw and SB cotton fibers after the heat treatment at 100 °C for 2 h. (e) UV/vis spectra of the control raw cotton fiber and raw cotton fiber treated at 80 °C and 100 °C for 2 h.

diagrams of the reduction reactions by cotton cellulose and pectin. The reduction of Ag cations was accomplished by oxidizing the hydroxyl-terminated chain ends of cellulose or pectin *via* duplicative acetaldehyde oxidation after cyclo-oxo tautomerization. Previous studies have investigated the ability of glucose and galacturonic acid units to reduce Ag ions to Ag atoms through simultaneous oxidation of the vicinal diols of the ring.[36,37] Pectin components, which contain a great number of reducing ends can remarkably contribute to the reduction reaction.[38] Moreover, pectin is capable of undergoing decarboxylation, which may result in the formation of dialdehydes. Dialdehydes can further reduce Ag ions to Ag atoms.

Conversely, cellulose has a small number of reducing ends because of its high degree of polymerization, *i.e.*, approximately 20 000 glucose units.[39] Therefore, the reduction reaction by cellulose is negligible.

Fig. 3a and b show the optical microscopic images of the longitudinal views of raw and SB cotton fibers after the heat treatment. The brown coloration was clearly observed on the individual raw cotton fiber under an optical microscope; however, it was not apparent on the SB cotton fibers. By closely observing a single raw cotton fiber, the brown color was not evenly distributed along the fiber length and across the fiber diameter. The brown color was more saturated on the groove
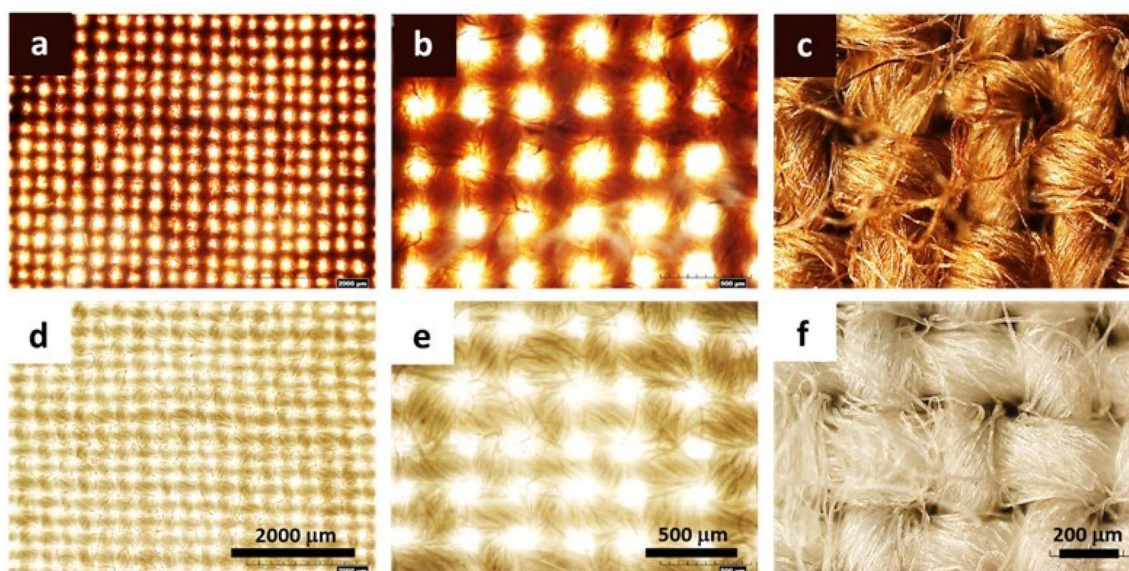

Fig. 4 Optical microscopic images at incremental magnifications for (a–c) raw and (d–f) SB cotton woven fabrics after the heat treatment at 100 °C for 2 h.
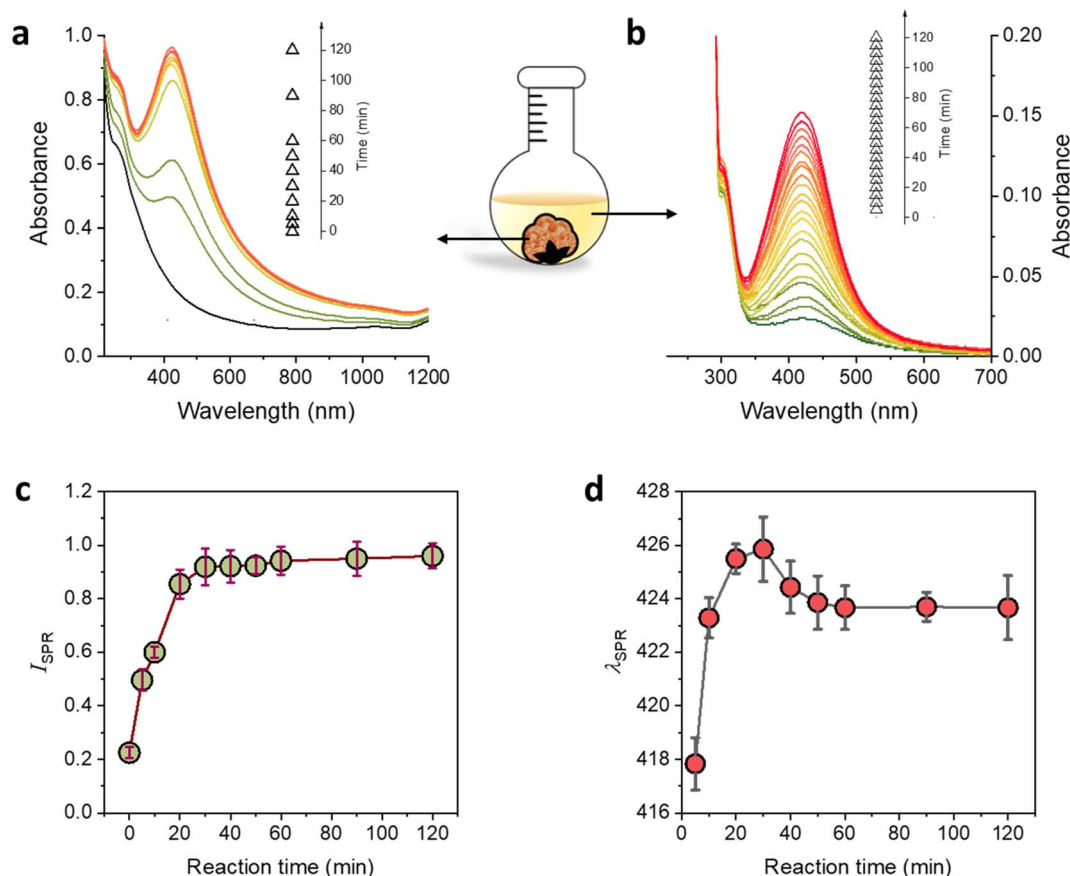
Fig. 5 UV/vis spectra of (a) raw cotton and (b) the reaction solution as a function of the reaction time at 100 °C. The insets show time intervals of measurement. (c) SPR intensities (I_{SPR}) and (d) wavelengths at the SPR maximum absorbance (λ_{SPR}) for raw cotton fiber measured at incremental reaction times at 100 °C.

area of the fiber (Fig. 3c), which is created when the living protoplast in the lumen dries out. The concentrations of Ag measured in the raw and SB cottons were 2261 and 41 mg kg^{-1}, respectively (Fig. 3d). The greater efficiency of the raw cotton woven fabric in producing Ag NPs was also demonstrated by obtaining optical microscopic images at various magnifications (Fig. 4a–f). The ability of raw cotton to produce Ag NPs decreased when the temperature was decreased to 80 °C. Fig. 3e shows that the SPR intensity of raw cotton fiber obtained at 80 °C was approximately 36% of the intensity obtained at 100 °C. Therefore, temperature is an important factor in the production of Ag NPs by raw cotton.

The production of Ag NPs using raw cotton was monitored by observing the corresponding UV/vis spectra of raw cotton fiber during the reaction at 100 °C for up to 2 h. Fig. 5a shows that the raw cotton fiber developed an SPR peak after only 5 min of the reaction, and the peak further developed, showing a certain pattern with the increase in the reaction time. Fig. 5b shows that the reaction solution also exhibited a weak SPR peak, whose intensity gradually increased with the increase in the reaction time. Fig. 5c shows the dependence of the SPR intensity of raw cotton on the reaction time. The SPR intensity rapidly increased during the first 20 min of the reaction, then gradually increased during the remaining reaction time (2 h). This two-

step increasing pattern is different from the three-step pattern observed in other studies that synthesized Ag NPs in bulk solutions containing reducing and stabilizing agents.[40–42] The three-step SPR evolution has been associated with an Ag NP formation mechanism involving three stages: (1) nuclei growth, (2) particle coalescence, and (3) Ostwald ripening. The second stage (particle coalescence), which induces rapid particle growth, is identified with the steepest increase in the SPR intensity. The Ostwald ripening stage, in which small particles dissolve and deposit onto large particles, is characterized by a slow increase in the SPR intensity. The plot of the wavelength at the SPR maximum absorbance (λ_{SPR}) as a function of the reaction time also indicates the transition from the second to the third stage (Fig. 5d). The SPR peak red-shifted in the second stage, whereas the SPR peak slightly blue shifted and then remained constant in the third stage. The first stage of nuclei growth, which occurs immediately after the addition of Ag atoms, was not detected in this study.

The optical properties of the raw cotton fiber resulting from the in situ synthesis of Ag NPs were examined by measuring the CIELAB color coordinates. Fig. 6a shows L^* as a function of the reaction time. The L^* of the raw cotton decreased with the increase in the reaction time until it reaches 30 min; however, no remarkable change was observed after that. The lightness of
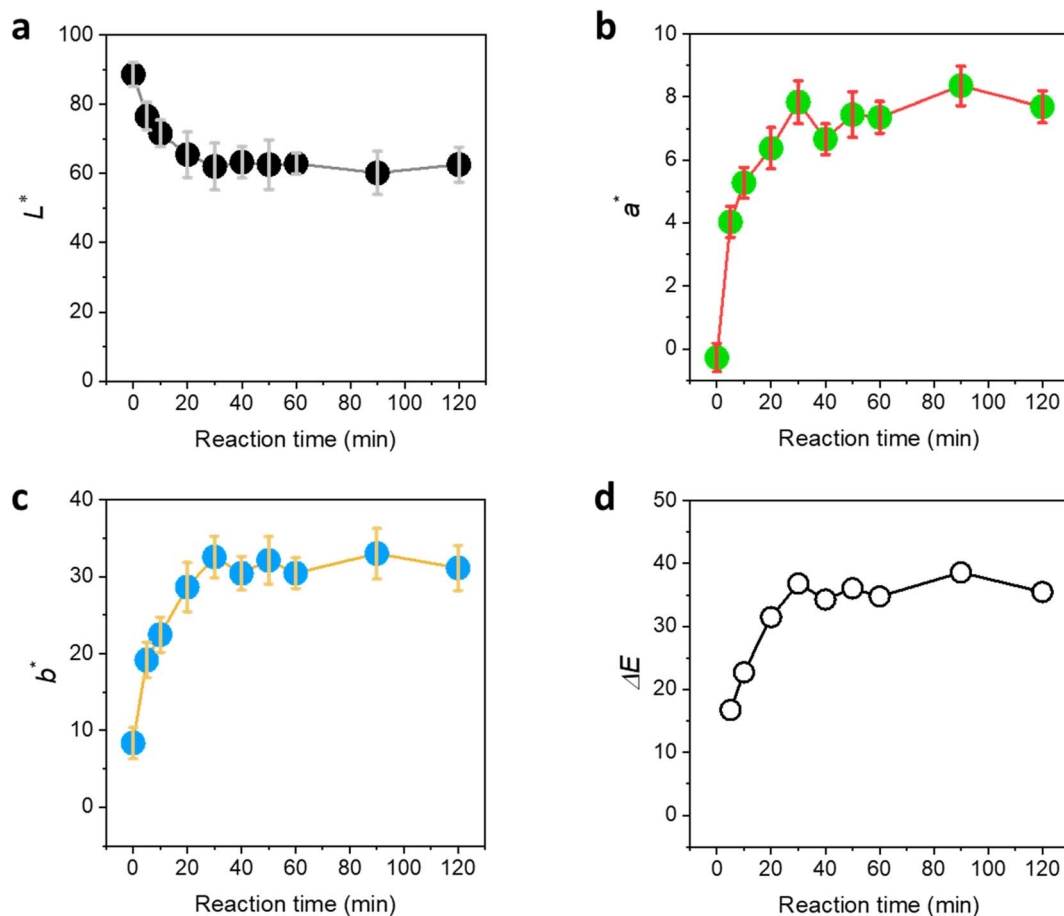
Fig. 6 CIELAB color coordinates: (a) L^*, (b) a^*, and (c) b^* for raw cotton as a function of the reaction time at 100 °C. (d) Color difference (ΔE^*) from the color coordinates of control raw cotton calculated by eqn (1) as a function of the reaction time at 100 °C.

raw cotton dropped by approximately 30% after the Ag NP synthesis. Both a^* (redness) and b^* (yellowness) of the raw cotton increased with the increase in the reaction time until it reached 30 min and remained steady for longer reaction times (Fig. 6b and c, respectively). The plot of the color difference (ΔE^*) calculated by eqn (2) shows that the maximum difference occurred after only 30 min of the reaction. The color of Ag NP-raw cotton differed from the color of control raw cotton by at most 36%.

To examine how Ag NPs were formed in the raw cotton, the cross-section of the fiber was observed using TEM. Fig. 7a–f show the TEM images of the fibers at different magnifications. Numerous Ag NPs were located in the outer wall of the raw cotton fiber. Mature cotton fiber has a hierarchical structure composed of the cuticle, primary wall, secondary, and lumen. Underlying the waxy cuticle is the primary cell wall (also called the outer wall), which is generally <0.5 μm thick.[43] Fig. 7d shows the primary cell wall, of which the thickness is approximately 200 nm. The outer wall contains various reducing noncellulosic constituents, such as pectin and sugars. According to a study using antibody probes, the primary cell wall also contains hemicellulose (mainly in the form of xyloglucan) in its inner-most layer.[44] The primary alcohols, secondary alcohols, and

diethers in hemicellulose can reduce Ag ions.[45] The TEM images also reveal that some Ag NPs were present in the secondary cell wall. The secondary cell wall is primarily composed of cellulose chains, which have weak reducing properties. The Ag NPs produced in the primary cell wall might diffuse into the secondary cell wall. The Ag NPs were individually dispersed inside the cotton fiber. Even though stabilizing agents were not used, no particle aggregation occurred. This controlled synthesis was attributed to the unique environment within the cotton fiber. When cotton fiber (diameter ≈ 20 μm) swells in water, its cross-sectional area increases by approximately 30%.[46] The opened microfibrillar structure creates nanosized channels, which improve heat and mass transfer within the structure. Furthermore, particles growing on the surface of the fiber structural elements are less likely to aggregate compared to those in a bulk solution. Previous research found that the internal formation of Ag NPs within cotton fibers slightly reinforced the tensile strength of the fiber[47] and increased the thermal sensitivity of cotton fiber during thermal decomposition and post heat treatment.[48]

Fig. 8a and b show the high-resolution TEM images of Ag NPs in the primary cell wall, and Fig. 8c and d show the images of Ag NPs in the secondary cell wall. The NPs in both the
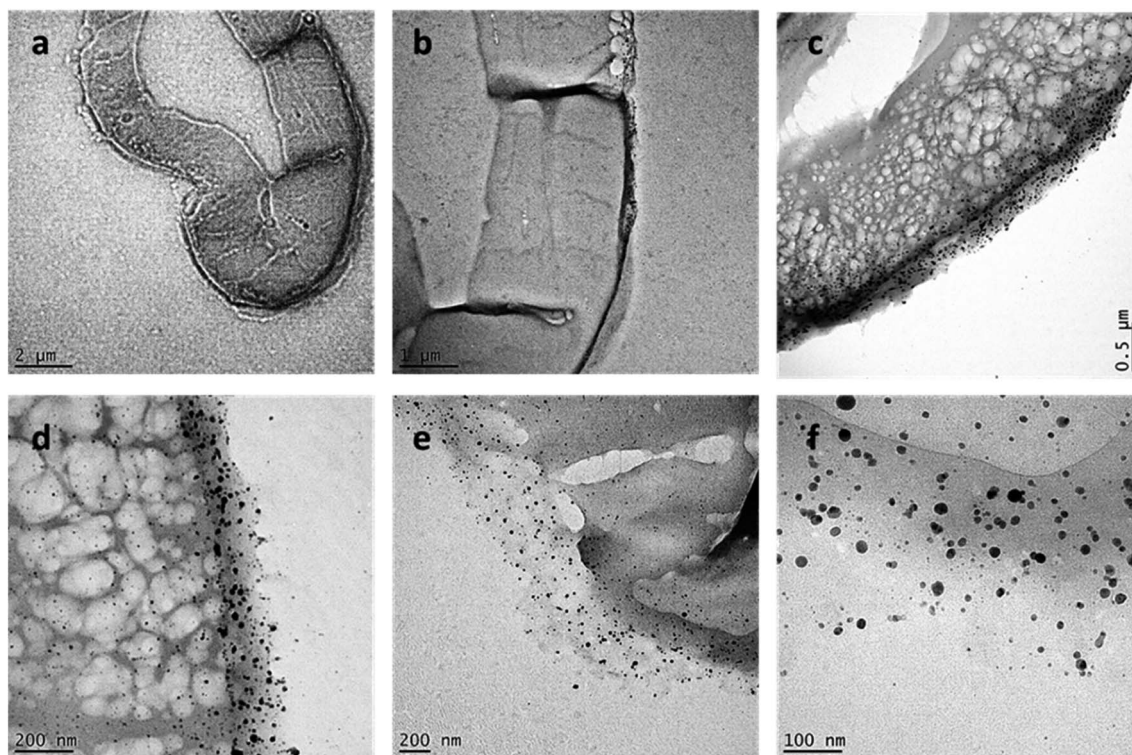
Fig. 7   (a–f) TEM images of the cross-section of Ag NP-raw cotton fiber at incremental magnifications showing the *in situ* synthesis of Ag NPs in the primary and secondary cell walls of raw cotton fiber.

primary and secondary walls are sphere-like. The images of the single Ag NPs (Fig. 8b and d) show that an individual particle contains several boundaries, at which lattice fringes are joined together at different angles. The *d*-spacings were determined based on some of the defined lattice fringes being 0.271 nm. Ag NPs grew through the coalescence of smaller crystalline particles. Ag NPs generated by a typical chemical synthesis in a bulk solution generally exhibit a decahedral structure.[42] Some particles synthesized in the raw cotton exhibited irregular structures. This heterogeneous structure was attributed to the unique environment, in which the particles grow. Unlike in the bulk solution, the nucleation and nuclei growth inside the cotton fiber are likely to occur on the surface of the fiber structural elements, which hinders the homogeneous particle collision and consequently the particle growth. Fig. 8e and f show the histograms of the particle diameter measured in the primary and secondary cell walls, respectively. Both size distributions were unimodal and followed the Gaussian distribution at $p = 0.127$ and $p = 0.067$, respectively, based on the Shapiro–Wilk test. The size distribution in the secondary cell wall shifted to lower values compared to that in the primary cell wall. The mean diameters measured in the primary and secondary cell walls were 27.8 ± 8.9 and 20.5 ± 7.4 nm, respectively. The higher number of reducing sites present in the primary cell wall compared to the secondary wall facilitated particle growth, producing larger particles. The XRD pattern confirmed that the generated NPs consisted of Ag elements. The XRD pattern of the control raw cotton fabric shows four 2θ peaks at 14.6°, 16.4°,

22.6°, and 34.4°, which are assigned to the (1−10), (110), (200), and (004) crystal planes of cellulose Iβ (Fig. 8g).[49] After the *in situ* synthesis of Ag NPs, the raw cotton exhibits strong additional peaks at 38.1°, 44.1°, 64.5°, and 77.4°, which were assigned to the (111), (200), (220), and (311) planes, respectively, of a face-centered cubic Ag crystal according to the database of the Joint Committee on Powder Diffraction Standards file no. 04-0783. The crystal sizes calculated by eqn (1) of the Ag NPs and cellulose were 7.8 and 5.6 nm, respectively.

The antimicrobial properties of the developed Ag NP-raw cotton were examined to confirm the superiority of raw cotton in generating and hosting Ag NPs compared to that of SB cotton. Ag NPs have powerful antimicrobial properties against broad-spectrum bacteria.[50] The biocidal properties of Ag NPs result from their being a source of Ag ions, which deactivate cellular enzymes[51,52] and disable the replication ability of DNA.[53] The large particle surface area of Ag NPs effectively promotes the release of Ag ions. Furthermore, Ag NPs themselves can physically damage the cell membrane[54–56] and cause oxidative stress to bacterial cells.[57,58] Fig. 9a and b show the percent viability reductions of *K. pneumonia* and *S. aureus* by raw and SB cotton fibers, respectively, as a function of the concentration of AgNO₃ in the *in situ* synthesis of Ag NPs. The antimicrobial activity of Ag NPs generated in cotton was so powerful that the contact time needed for bacterial destruction was reduced from 24 to 0.5 h. Raw cotton required lower concentrations of $AgNO_3$ than SB cotton to achieve a 99.99% reduction of Gram-negative and Gram-positive bacteria. In the case of *K. pneumonia*, the lowest
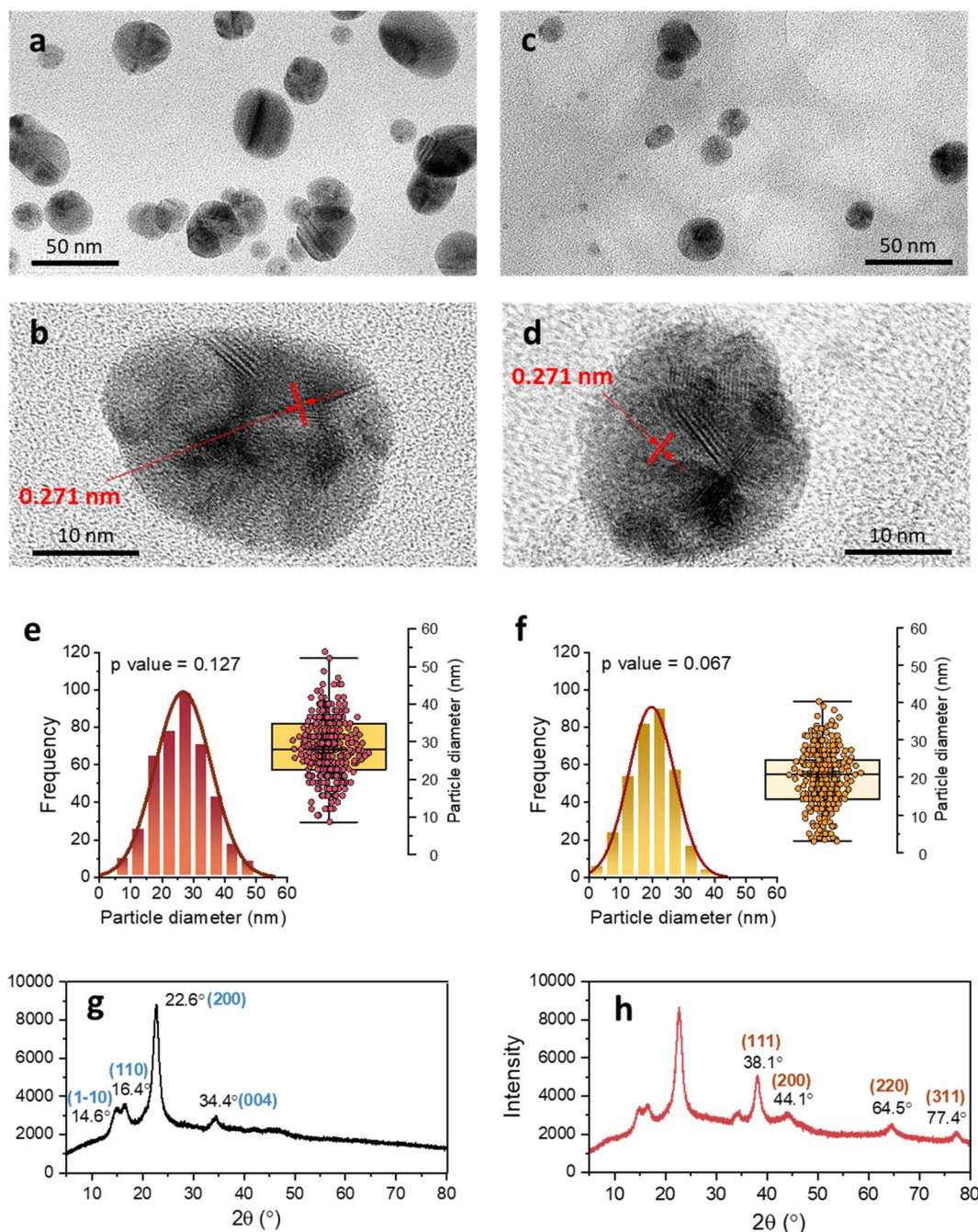
Fig. 8 High-resolution TEM images of Ag NPs taken in the (a and b) primary cell wall and (c and d) secondary wall. Lattice fringes with *d*-spacings were indicated with a red color. Histograms for the Ag NP diameter in the (e) primary cell wall and (f) secondary wall. The solid lines are Gaussian fits to the size distribution. The insets show the corresponding box plots of particle size. XRD patterns for (g) control cotton and (h) Ag NP-raw cotton fabrics.

concentration of $AgNO_3$ for raw cotton fiber to achieve a 99.99% reduction was ten times lower than that for SB cotton fiber. In case of *S. aureus*, SB cotton fiber exhibited only 41.6% viability reduction at the lowest concentration of $AgNO_3$ for raw cotton fiber to achieve a 99.99% reduction. The bacterial reductions on SB cotton fiber observed at the same concentrations of $AgNO_3$ are lower than those observed on raw cotton because SB cotton fiber does not contain noncellulosic components, which have active binding sites for Ag cations such as negatively charged

hydroxyl and carboxylic groups. Therefore, SB fiber cannot synthesize sufficient Ag NP, leading to poor antimicrobial properties. In contrast, Ag ions are readily adsorbed on raw cotton fiber, which has noncellulosic component, promoting the production of Ag NPs and thus lowering the lowest concentration of $AgNO_3$ to achieve a 99.99% reduction. This result confirmed that raw cotton fiber is a superior host for the Ag NP synthesis than SB cotton fiber.
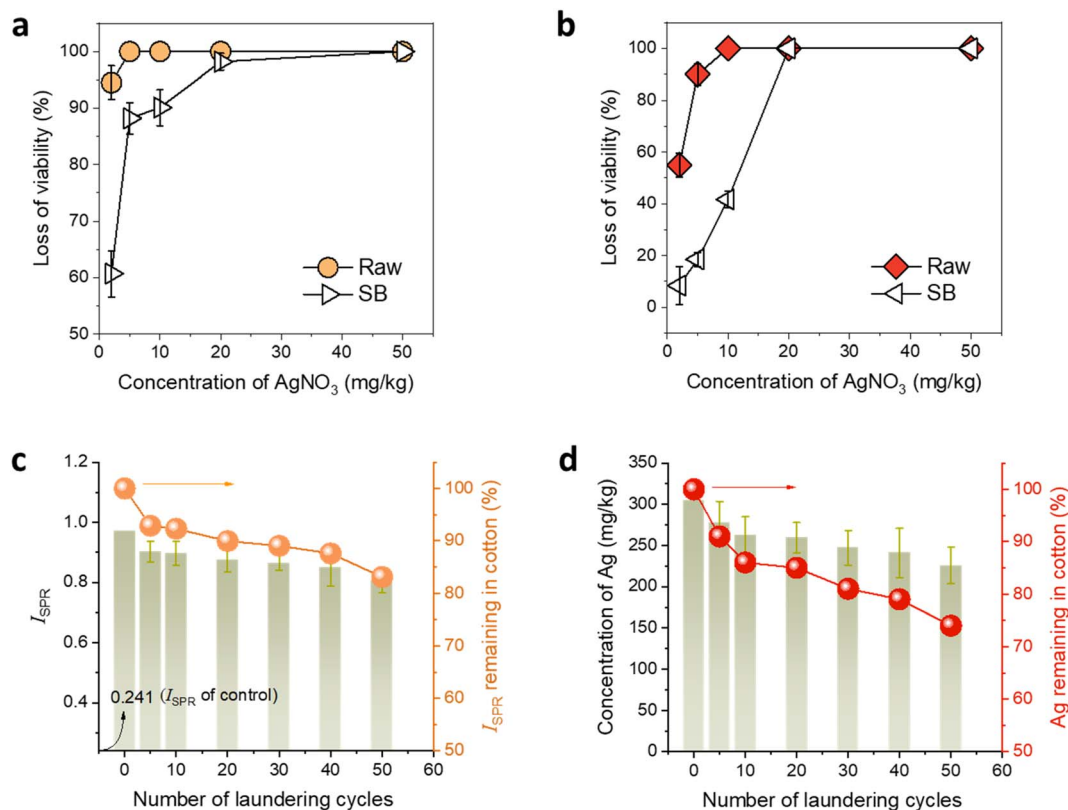
Fig. 9 Percent viability reductions of (a) *K. pneumonia* and (b) *S. aureus* on raw cotton and SB cotton fibers as a function of the concentration of AgNO₃ in the *in situ* synthesis of Ag NPs. Washing durability of Ag NP-raw cotton fabric prepared at 100 °C for 2 h: (c) intensity of the SPR absorption peak and (d) Ag concentration as a function of the number of laundering cycles.

Raw cotton is not only an efficient Ag NP producer but also a durable Ag NP binder. Once Ag NPs were synthesized by raw cotton, they hardly leached out of the fiber during laundering. Studies have reported that the Ag NP-treated textile products currently on the market lack Ag NP washing durability.[59–62] Even though some of these products used chemical binders, most of the NPs could not withstand the mechanical forces and/or surfactants used during washing in a laundry machine. Fig. 9c and d show the SPR intensity and concentration of Ag in Ag NP-raw cotton fabrics, respectively, as a function of the number of laundering cycles. The Ag NP-raw cotton fabric was prepared at 100 °C for 2 h. The concentration of Ag on the fabric (based on the dry weight of the fabric) was 2261 mg kg⁻¹. The SPR intensity dropped by approximately 7% after the initial five cycles, and the corresponding Ag content dropped by about 9%. With the increase in the number of laundering cycles, the SPR intensity and Ag concentration of the Ag NP-raw cotton fabric gradually decreased. After 50 cycles, the losses in the SPR intensity and Ag concentration were approximately 17% and 26%, respectively, showing that the majority of Ag NPs remained in the raw cotton. The *in situ* formed Ag NPs were physically anchored in the internal structure of the cotton fiber and electrostatically bound onto the oxygen-rich cellulose and noncellulosic components.

Conclusions

In this study, a sustainable and affordable method was proposed to use nanotechnology for producing permanent antimicrobial textile products. The current nanotechnology used in the textile industry involves complex and high-cost synthesis of silver nanoparticles (Ag NPs), and the Ag NP-treated textile products are not durable. Here, it was confirmed that raw cotton fiber can readily synthesize Ag NPs *in situ* (2261 mg kg⁻¹) without any reducing or stabilizing agents. Unlike scoured and bleached (SB) cotton, which is typically used in the fabrication of textiles, raw cotton contains noncellulosic constituents in the primary cell wall, which act as reducing agents. TEM images of the cross-section of the fiber confirmed the 200 nm – thick inorganic–organic substructure, in which many Ag NPs (diameter ≈ 28 nm) were individually dispersed. Some Ag NPs diffuse into the secondary cell wall. The Ag NPs synthesized underneath the fiber surface were physically trapped and chemically bound to the internal structure of the fiber, exhibiting superior washing durability. Approximately 74% of the total Ag in the raw cotton fabric remained after 50 laundering cycles. The Ag NP synthesis by raw cotton fiber is economical and ecofriendly because it eliminates the need for reducing and stabilizing agents as well as binders and saves large amounts of water, energy, and chemicals that are used in

the scouring and bleaching processes. This nanostructured raw cotton fiber can be blended in the nonwoven or woven fabrication, producing durable antimicrobial textile products.

Conflicts of interest

The authors declare no conflict of interest. Mention of trade names or commercial products in this publication is solely for the purpose of providing specific information and does not imply recommendation or endorsement by the U.S. Department of Agriculture. USDA is an equal opportunity provider and employer.

References

1 S. Khan, S. Mansoor, Z. Rafi, B. Kumari, A. Shoaib, M. Saeed, S. Alshehri, M. M. Ghoneim, M. Rahamathulla, U. Hani and F. Shakeel, A review on nanotechnology: Properties, applications, and mechanistic insights of cellular uptake mechanisms, *J. Mol. Liq.*, 2022, **348**, 118008.

2 G. Grasso, D. Zane and R. Dragone, Microbial nanotechnology: Challenges and prospects for green biocatalytic synthesis of nanoscale materials for sensoristic and biomedical applications, *Nanomaterials*, 2019, **10**(1), 11.

3 F. D. Guerra, M. F. Attia, D. C. Whitehead and F. Alexis, Nanotechnology for environmental remediation: Materials and applications, *Molecules*, 2018, **23**, 1760.

4 M. A. Shah, B. M. Pirzada, G. Price, A. L. Shibiru and A. Qurashi, Applications of nanotechnology in smart textile industry: A critical review, *J. Adv. Res.*, 2022, **38**, 55–75.

5 M. Fernandes, J. Padrao, A. I. Ribeiro, R. D. V. Fernandes, L. Melro, T. Nicolau, B. Mehravani, C. Alves, R. Rodrigues and A. Zille, Polysaccharides and metal nanoparticles for functional textiles: A review, *Nanomaterials*, 2022, **12**(6), 1006.

6 F. Fievet, J. P. Lagier, B. Blin, B. Beaudoin and M. Figlarz, Homogeneous and heterogeneous nucleations in the polyol process for the preparation of micron and sub-micron size metal particles, *Solid State Ionics*, 1989, **32–33**, 198–205.

7 F. Fiévet, J. P. Lagier and M. Figlarz, Preparing monodisperse metal powders in micrometer and submicrometer sizes by the polyol process, *MRS Bull.*, 1989, **14**, 29–34.

8 H. R. El-Seedi, R. M. El-Shabasy, S. A. M. Khalifa, A. Saeed, A. Shah, R. Shah, F. J. Iftikhar, M. M. Abdel-Daim, A. Omri, N. H. Hajrahand, J. S. M. Sabir, X. Zou, M. F. Halabi, W. Sarhan and W. Guo, Metal nanoparticles fabricated by green chemistry using natural extracts: biosynthesis, mechanisms, and applications, *RSC Adv.*, 2019, **9**, 24539–24559.

9 J. M. Palomo and M. Filice, Biosynthesis of Metal Nanoparticles: Novel Efficient Heterogeneous Nanocatalysts, *Nanomaterials*, 2016, **6**, 84.

10 T. S. Rodrigues, A. G. M. da Silva and P. H. C. Camargo, Nanocatalysis by noble metal nanoparticles: controlled synthesis for the optimization and understanding of activities, *J. Mater. Chem.*, 2019, **7**, 5857–5874.

11 A. V. Nikam, B. L. V. Prasad and A. A. Kulkarni, Wet chemical synthesis of metal oxide nanoparticles: A review, *Crystengcomm*, 2018, **20**, 5091–5107.

12 J. Niskanen, J. Shan, H. Tenhu, H. Jiang, E. Kauppinen, V. Barranco, F. Picó, K. Yliniemi and K. Kontturi, Synthesis of copolymer-stabilized silver nanoparticles for coating materials, *Colloid Polym. Sci.*, 2010, **288**, 543–553.

13 S. Y. Park, J. W. Chung, R. D. Priestley and S. Y. Kwak, Covalent assembly of metal nanoparticles on cellulose fabric and its antimicrobial activity, *Cellulose*, 2012, **19**, 2141–2151.

14 H. J. Lee, S. Y. Yeo and S. H. Jeong, Antibacterial effect of nanosized silver colloidal solution on textile fabrics, *J. Mater. Sci.*, 2003, **38**, 2199–2204.

15 M. H. El-Rafie, H. B. Ahmed and M. K. Zahran, Characterization of nanosilver coated cotton fabrics and evaluation of its antibacterial efficacy, *Carbohydr. Polym.*, 2014, **107**, 174–181.

16 K. Kulthong, S. Srisung, K. Boonpavanitchakul, W. Kangwansupamonkon and R. Maniratanachote, Determination of silver nanoparticle release from antibacterial fabrics into artificial sweat, *Part. Fibre Toxicol.*, 2010, **7**, 8.

17 C. Lorenz, L. Windler, N. von Goetz, R. P. Lehmann, M. Schuppler, K. Hungerbühler, M. Heuberger and B. Nowack, Characterization of silver release from commercially available functional (nano)textiles, *Chemosphere*, 2012, **89**, 817–824.

18 L. Geranio, M. Heuberger and B. Nowack, The behavior of silver nano textiles during washing, *Environ. Sci. Technol.*, 2009, **43**, 8113–8118.

19 T. M. Benn and P. Westerhoff, Nanoparticle silver released into water from commercially available sock fabrics, *Environ. Sci. Technol.*, 2008, **42**, 4133–4139.

20 T. Benn, B. Cavanagh, K. Hristovski, J. D. Posner and P. Westerhoff, The release of nanosilver from consumer products used in the home, *J. Environ. Qual.*, 2010, **39**, 1875–1882.

21 N. F. Attia and M. Mousa, Synthesis of smart coating for furniture textile and their flammability and hydrophobic properties, *Prog. Org. Coat.*, 2017, **110**, 204–209.

22 N. F. Attia, M. Moussa, A. M. F. Sheta, R. Taha and H. Gamal, Synthesis of effective multifunctional textile based on silicananoparticles, *Prog. Org. Coat.*, 2017, **106**, 41–49.

23 N. F. Attia, A. M. Eid, M. A. Soliman and M. Nagy, Exfoliation and decoration of graphene sheets with silver nanoparticles and their antibacterial properties, *J. Polym. Environ.*, 2018, **26**, 1072–1077.

24 N. F. Attia, A. Mohamed, A. Hussein, A. G. M. El-Demerdash and S. H. Kandil, Bio-inspired one-dimensional based textile fabric coating for integrating high flame retardancy, antibacterial, toxic gases suppression, antiviral and reinforcement properties, *Polym. Degrad. Stab.*, 2022, **205**, 110152.

25 N. F. Attia, H. E. Ahmed, A. A. El Ebissy and S. E. A. El Ashery, Green and novel approach for enhancing flame retardancy, UV protection and mechanical properties of fabrics

utilized in historical textile fabrics conservation, *Prog. Org. Coat.*, 2022, **166**, 106822.

26 H. L. Chen and L. D. Burns, Environmental analysis of textile products, *Cloth. Text. Res. J.*, 2006, **24**, 248–261.

27 G. Baydar, N. Ciliz and A. Mammadov, Life cycle assessment of cotton textile products in Turkey, *Resour., Conserv. Recycl.*, 2015, **104**, 213–223.

28 D. P. Thibodeaux and J. P. Evans, Cotton fiber maturity by image analysis, *Text. Res. J.*, 1986, **56**, 130–139.

29 E. K. Boylston, O. Hinojosa and J. J. Hebert, A quick embedding method for light and electron microscopy of textile fibers, *Biotech. Histochem.*, 1991, **66**(3), 122–124.

30 C. A. Schneider, W. S. Rasband and K. W. Eliceiri, NIH Image to ImageJ: 25 years of image analysis, *Nat. Methods*, 2012, **9**, 671–675.

31 P. Scherrer, Bestimmung der Grösse und der inneren Struktur von Kolloidteilchen mittels Röntgenstrahlen, *Nachr. Ges. Wiss. Goettingen*, 1918, **26**, 98–100.

32 J. I. Langford and A. J. C. Wilson, Scherrer after sixty years: A survey and some new results in the determination of crystallite size, *J. Appl. Crystallogr.*, 1978, **11**, 102–113.

33 S. Levy, *Meet fibers' green dream team*, 2010, accessed 11.16, **https:\\www.cottoninc.com/product/NonWovens/ Nonwoven-News/NonwovenNewsArticles/2010/Fibers-Green-Dream-Team**.

34 L. Gary, K. Osteen, R. Johnson and S. Johnson, *True cotton nonwoven fibres*, 2014, accessed 11.16, **https:// www.cottoninc.com/product/nonwovens/nonwoven-news/ nonwovennewsarticles/2014/techtex-india**.

35 D. J. Hinchliffe, A. De Lucca, B. Condon, J. O'Regan, J. Clemmons, L. Zeng, R. K. Byler, M. Reynolds, H. Allen, M. Santiago Cintrón and C. Madison, A pilot-scale nonwoven roll goods manufacturing process reduces microbial burden to pharmacopeia acceptance levels for non-sterile hygiene applications, *Text. Res. J.*, 2014, **84**, 546–558.

36 P. Pallavicini, C. R. Arciola, F. Bertoglio, S. Curtosi, G. Dacarro, A. D'Agostino, F. Ferrari, D. Merli, C. Milanese, S. Rossi, A. Taglietti, M. Tenci and L. Visai, Silver nanoparticles synthesized and coated with pectin: An ideal compromise for anti-bacterial and anti-biofilm action combined with wound-healing properties, *J. Colloid Interface Sci.*, 2017, **498**, 271–281.

37 M. K. Zahran, H. B. Ahmed and M. H. El-Rafie, Facile size-regulated synthesis of silver nanoparticles using pectin, *Carbohydr. Polym.*, 2014, **111**, 971–978.

38 K. Hileuskaya, A. Ladutska, V. Kulikouskaya, A. Kraskouski, G. Novik, I. Kozerozhets, A. Kozlovskiy and V. Agabekov, 'Green' approach for obtaining stable pectin-capped silver nanoparticles: Physico-chemical characterization and antibacterial activity, *Colloids Surf., A*, 2020, **585**, 124141.

39 P. J. Wakelyn, N. R. Bertoniere, A. D. French, D. P. Thibodeaux, B. A. Triplett, M. Rousselle, W. R. Goynes Jr, J. V. Edwards, L. Hunter, D. D. McAlister and G. R. Gamble, *Cotton Fiber Chemistry and Technology*, CRC Press, Boca Raton, 2006.

40 P. Y. Silvert, R. Herrera-Urbina and K. Tekaia-Elhsissen, Preparation of colloidal silver dispersions by the polyol process. 2. Mechanism of particle formation, *J. Mater. Chem.*, 1997, **7**, 293–299.

41 A. Slistan-Grijalva, R. Herrera-Urbina, J. F. Rivas-Silva, M. Avalos-Borja, F. F. Castillon-Barraza and A. Posada-Amarillas, Assessment of growth of silver nanoparticles synthesized from an ethylene glycol-silver nitrate-polyvinylpyrrolidone solution, *Phys. E*, 2005, **25**, 438–448.

42 S. Nam, B. Park and B. D. Condon, Water-based binary polyol process for the controllable synthesis of silver nanoparticles inhibiting human and foodborne pathogenic bacteria, *RSC Adv.*, 2018, **8**, 21937–21947.

43 J. M. Maxwell, S. G. Gordon and M. G. Huson, Internal structure of mature and immature cotton fibers revealed by scanning probe microscopy, *Text. Res. J.*, 2003, **73**, 1005–1012.

44 K. C. Vaughn and R. B. Turley, The primary walls of cotton fibers contain an ensheathing pectin layer, *Protoplasma*, 1999, **209**, 226–237.

45 X. Lin, J. Zhao, M. Wu, S. Kuga and Y. Huang, Green synthesis of gold, platinum and palladium nanoparticles by lignin and hemicellulose, *J. Microbiol. Biotechnol.*, 2016, **5**, 14–18.

46 A. T. Moore, L. W. Scott, I. V. deGruy and M. L. Rollins, The swelling of cotton in water: A microscopical study, *Text. Res. J.*, 1950, **20**, 620–630.

47 S. Nam, B. D. Condon, C. D. Delhom and K. R. Fontenot, Silver-cotton nanocomposites: Nano-design of microfibrillar structure causes morphological changes and increased tenacity, *Sci. Rep.*, 2016, **6**, 37320.

48 S. Nam, I. S. Baek, M. B. Hillyer, Z. He, J. Y. Barnaby, B. D. Condon and M. S. Kim, Thermosensitive textiles made from silver nanoparticle-filled brown cotton fibers, *Nanoscale Adv.*, 2022, **4**, 3725–3736.

49 A. D. French, Idealized powder diffraction patterns for cellulose polymorphs, *Cellulose*, 2014, **21**, 885–896.

50 M. K. Rai, S. D. Deshmukh, A. P. Ingle and A. K. Gade, Silver nanoparticles: the powerful nanoweapon against multidrug-resistant bacteria, *J. Appl. Microbiol.*, 2012, **112**, 841–852.

51 A. Gupta, M. Maynes and S. Silver, Effects of halides on plasmid-mediated silver resistance in Escherichia coli, *Appl. Environ. Microbiol.*, 1998, **64**, 5042–5045.

52 Y. Matsumura, K. Yoshikata, S. Kunisaki and T. Tsuchido, Mode of bacterial action of silver zeolite and its comparison with that of silver nitrate, *Appl. Environ. Microbiol.*, 2003, **69**, 4278–4281.

53 Q. L. Feng, J. Wu, G. Q. Chen, F. Z. Cui, T. N. Kim and J. O. Kim, A mechanistic study of the antibacterial effect of silver ions on Escherichia coli and Staphylococcus aureus, *J. Biomed. Mater. Res.*, 2000, **52**(4), 662–668.

54 A. Dror-Ehre, H. Mamane, T. Belenkova, G. Markovich and A. Adin, Silver nanoparticle-E. coli collodial interaction in water and effect on E. coli survival, *J. Colloid Interface Sci.*, 2009, **339**(2), 521–526.

55 A. M. El Badawy, R. G. Silva, B. Morris, K. G. Scheckel, M. T. Suidan and T. M. Tolaymat, Surface charge-

dependent toxicity of silver nanoparticles, *Environ. Sci. Technol.*, 2011, **45**(1), 283–287.

56 J. R. Morones, J. L. Elechiguerra, A. Camacho, K. Holt, J. B. Kouri, J. T. Ramirez and M. J. Yacaman, The bactericidal effect of silver nanoparticles, *Nanotechnology*, 2005, **16**, 2346–2353.

57 C. Carlson, S. M. Hussain, A. M. Schrand, L. K. Braydich-Stolle, K. L. Hess, R. L. Jones and J. J. Schlager, Unique cellular interaction of silver nanoparticles: size-dependent generation of reactive oxygen species, *J. Phys. Chem. B*, 2008, **112**, 13608–13619.

58 O. Choi and Z. Hu, Size dependent and reactive oxygen species related nanosilver toxicity to nitrifying bacteria, *Environ. Sci. Technol.*, 2008, **42**, 4583–4588.

59 D. M. Mitrano, E. Rimmele, A. Wichser, R. Erni, M. Height and B. Nowack, Presence of nanoparticles in wash water from conventional silver and nano-silver textiles, *ACS Nano*, 2014, **8**(7), 7208–7219.

60 P. Limpiteeprakan, S. Babel, J. Lohwacharin and S. Takizawa, Release of silver nanoparticles from fabrics during the course of sequential washing, *Environ. Sci. Pollut. Res. Int.*, 2016, **23**(22), 22810–22818.

61 H. Liu, M. Lv, B. Deng, J. Li, M. Yu, Q. Huang and C. Fan, Laundering durable antibacterial cotton fabrics grafted with pomegranate-shaped polymer wrapped in silver nanoparticle aggregations, *Sci. Rep.*, 2014, **4**, 5920.

62 J. Zhou, D. Cai, Q. Xu, Y. Zhang, F. Fu, H. Diao and X. Liu, Excellent binding effect of l-methionine for immobilizing silver nanoparticles onto cotton fabrics to improve the antibacterial durability against washing, *RSC Adv.*, 2018, **8**(43), 24458–24463.